Supporting Information for the manuscript entitled

Enhanced Li^+ ion transport in $LiNi_{0.5}Mn_{1.5}O_4$ through Control of Site Disorder

Jianming Zheng,[a] Jie Xiao,*[a] Xiqian Yu,[b] Libor Kovarik,[a] Meng Gu,[a] Fredrick Omenya,[c] Xiao-Qing Yang,[b] Jun Liu,[a] Gordon L. Graff,[a] M. Stanley Whittingham[c] and Ji-Guang Zhang*[a]

[a], Energy and Environment Directorate, Pacific Northwest National Laboratory, Richland, WA 99352, USA

[b], Chemistry Department, Brookhaven National Laboratory, Upton, NY, 11973, USA

[c], Department of Chemistry, State University of New York at Binghamton (SUNY Binghamton), New York 13902, USA

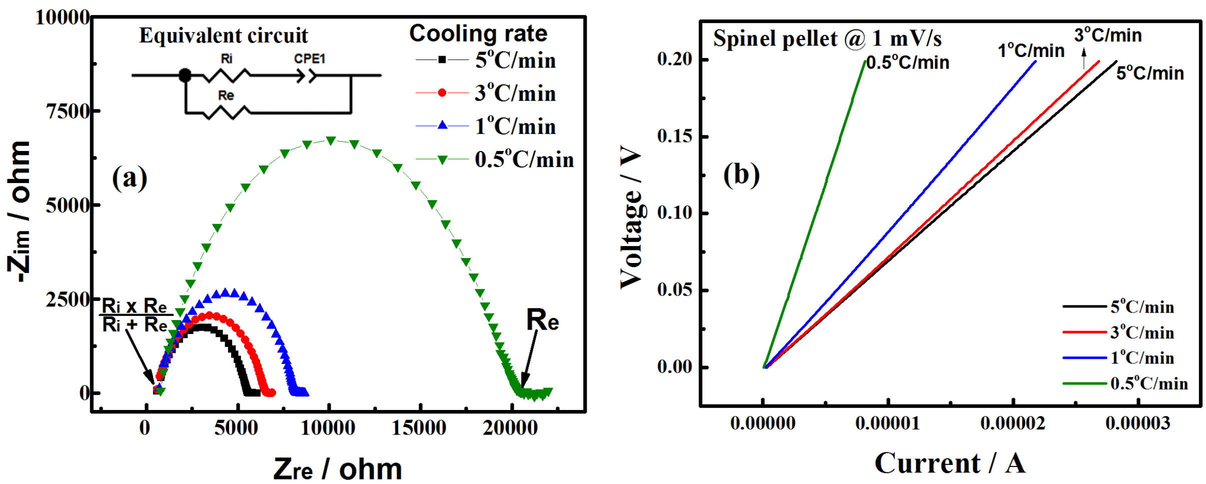

Figure S1. (a) Nyquist plots and (b) V/I curves of $LiNi_{0.5}Mn_{1.5}O_4$ pellets prepared with different cooling rates. The inset is the equivalent circuit for mixed conductive materials. Detailed parameters of pellets for conductivity test and results of the ionic and electronic conductivities are shown as follows. Electronic conductivities measured by two methods are consistent.

Cooling rate	5°C/min	3°C/min	1°C/min	0.5°C/min
Pellet thickness / cm	0.082	0.092	0.098	0.087
Diameter / cm	0.80	0.95	0.95	0.93
σ_i from EIS	2.40×10^{-4}	2.28×10^{-4}	2.19×10^{-4}	1.78×10^{-4}
σ_e from EIS	2.85×10^{-5}	1.95×10^{-5}	1.66×10^{-5}	0.70×10^{-5}
σ_e from linear voltage scan	2.26×10^{-5}	1.72×10^{-5}	1.49×10^{-5}	0.52×10^{-5}

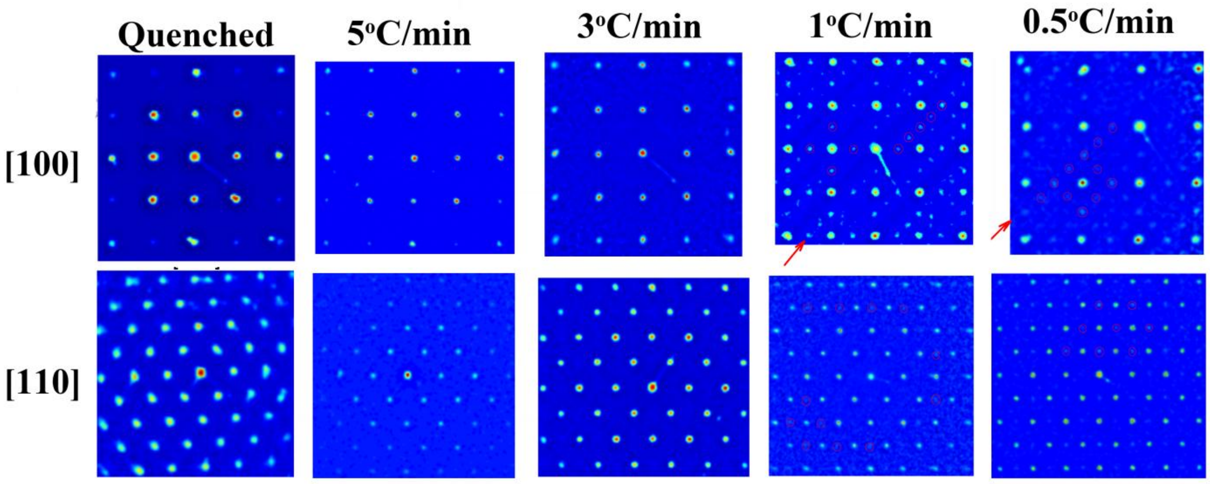

Figure S2. Electron diffraction patterns of $LiNi_{0.5}Mn_{1.5}O_4$ prepared with different cooling rates. The diffraction patterns are plotted in log-scale and then filtered using a bandpass filter to clean the background noise and show the weak superlattice peaks more clearly. Supperlattice peaks are circled in red. When cooled at 1°C/min, extra diffraction pattern caused by Ni/Mn ordering can be clearly seen. More superlattice dots are observable around the typical spinel diffraction at a slower cooling rate of 0.5°C/min.

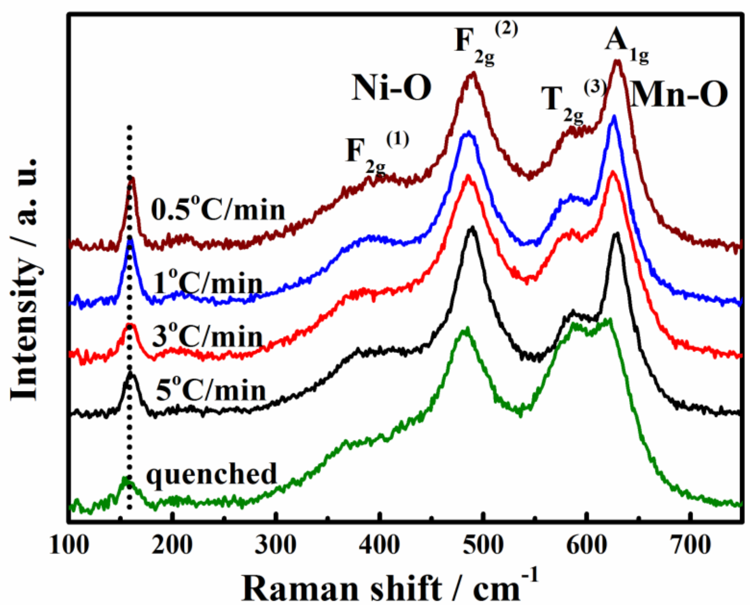

Figure S3. Raman spectra of $LiNi_{0.5}Mn_{1.5}O_4$ prepared with different cooling rates. Both peaks at about 400 ($F_{2g}^{(1)}$) and 490 cm^{-1} ($F_{2g}^{(2)}$) are associated with Ni^{2+}-O stretching mode in the spinel structure. The strong band at around 630 cm^{-1} is due to the symmetric Mn-O stretching mode of MnO_6 octahedra (A_{1g}). With the decrease of cooling rate, the peaks (especially the peak at ca. 161 cm^{-1}) for slower cooled sampled is sharper than the faster cooled sample. The strong peak at 161 cm^{-1} is the feature of $P4_332$ structure (ordered phase). It could be concluded that the slow cooling rate is in favor of the formation of ordered spinel.

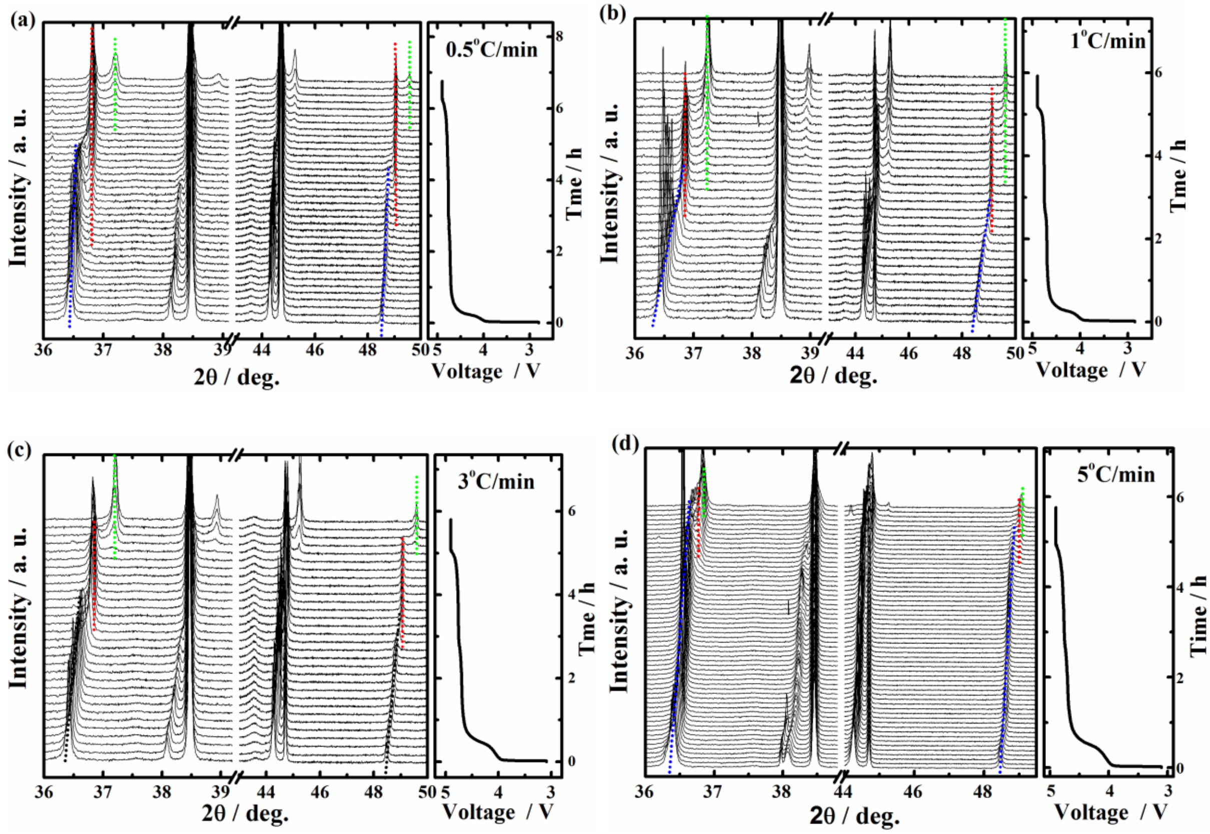

Figure S4. In-situ XRD patterns and corresponding charge curves of $LiNi_{0.5}Mn_{1.5}O_4$ prepared with cooling rates of (a) 0.5°C/min; (b) 1°C/min; (c) 3°C/min and (d) 5°C/min. The faster cooled spinel has more disordered phase/Mn^{3+} in the lattice and longer range of solid solution reaction during initial charge processes.

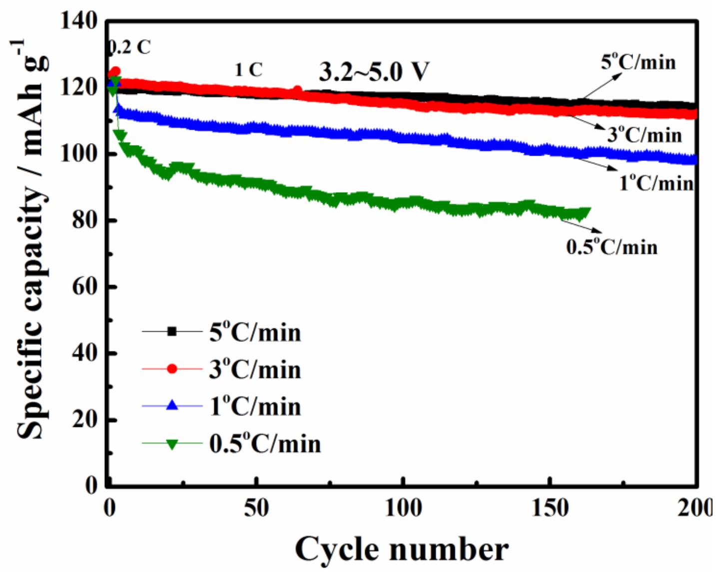

Figure S5. Cycling performance for $LiNi_{0.5}Mn_{1.5}O_4$ prepared with different cooling rates at 1 C after initial charge/discharge at 0.2 C for 2 cycles. Cycling performance tests performed on duplicate $Li/LiNi_{0.5}Mn_{1.5}O_4$ cells again demonstrates that the spinel with high cooling rate (5°C/min) shows superior cycling stability over the other spinels with lower cooling rate.